Desalination and Water Treatment
www.deswater.com
doi: 10.5004/dwt.2022.29078

278 (2022) 129–140
December

Rapid uptake of Pb(II) in water by β-cyclodextrin functionalized sycamore leaf-based biochar

Xiangyi Gong[a,b,*], Fengying Wu[a,b], Zeya Wang[a], Dekang Meng[a], Dajun Ren[a]

[a]*School of Resource and Environmental Engineering, Wuhan University of Science and Technology, Wuhan 430081, China, emails: gxywust@163.com (X. Gong), 18389585372@163.com (F. Wu), 13507282990@139.com (Z. Wang), 295944628@qq.com (D. Meng), dj_ren@163.com (D. Ren)*
[b]*Hubei Key Laboratory for Efficient Utilization and Agglomeration of Metallurgic Mineral Resources, Wuhan University of Science and Technology, Wuhan 430081, China*

Received 30 April 2022; Accepted 25 October 2022

ABSTRACT

A novelty and economy of β-cyclodextrin (β-CD) functionalized sycamore leaf-based biochar (BC) was synthesized, namely β-BC, and was used to study the potential adsorption mechanism of Pb(II) in water. Through scanning electron microscopy, Brunauer–Emmett–Teller, Fourier-transform infrared spectroscopy and X-ray diffraction characterization analyses, it was confirmed that the β-CD was successfully loaded. A succession of kinetic adsorption, isothermal adsorption and influencing factor experiments were carried out. The results showed that when compared with BC, the time for β-BC to reach adsorption equilibrium was reduced by half, and the removal efficiency increased from 89.84% to 98.48%. Meanwhile, the optimal pH was 5.0 and the dosage of β-BC was 0.05 g. The pseudo-second model and Freundlich isotherm model fitted the adsorption process for β-BC well. The maximum adsorption of Pb(II) in a single system was 151.2 mg g^{-1}, and the adsorption of binary systems was 92.03 mg g^{-1}, it was proved that Cd(II) has exert a competitive effect on Pb(II). The results demonstrated that β-BC has efficient and fast removal of Pb(II), it was primarily attributed to electrostatic action, complexation, hydrogen bonding of a wealth of oxygenated groups on the surface, and host-object interaction in the β-CD cavity. This research confirmed the extraordinary potential of β-BC to treat heavy metals in wastewater.

Keywords: β-Cyclodextrin; Biochar; Pb^{2+}; Adsorption

1. Introduction

The prevailing emergence of smelting, electroplating, mining, battery manufacturing and other industries have resulted in a class of thousands of heavy metal pollutants such as lead, mercury, cadmium and cobalt [1,2]. Notwithstanding the heavy metal ions appears in a fraction of concentrations, with migration and aggregation accumulating, their concealment and delay are reinforced capable of engendering severe and irreversible damage to life in nature [3,4]. According to the U.S. Environmental Protection Agency, the concentration of Pb^{2+} is elevated to 8 Í 10^{-8} g mL^{-1} in the body, it can adversely affect children's nerves, intelligence, hematopoietic ability, and hearing, meanwhile it also increases the risk of cardiovascular disease even death [5]. This trend is not necessarily unexpected how to effectively remove Pb^{2+} with ultrahigh biotoxicity and non-biodegradability. Currently, the main removal methods include chemical reaction, membrane separation, microbial flocculation, ion exchange and adsorption [6]. Among them, ion exchange technology uses heavy metal ions and ionic resins to exchange ions to achieve wastewater treatment [7]. Its limitations are reflected in the strength and durability of ion exchange resins [8]. Phytoremediation is classified as plant-based as receptors were applied to repair polluted soil and water, however, its development

* Corresponding author.

is restricted in many aspects, and scientists trying to combine other technologies with phytoremediation may be a breakthrough [9]. Noteworthy, adsorption makes use of the characteristics of adsorbents to actualize immobilization of multi-pollutants [10,11], it is extensively applied to pollutants owning to the feature of low-cost and high-efficiency, simple operation, and no secondary pollution. So far, it has been well documented that activated carbon, fly ash, bentonite and other adsorbents significantly dislodge heavy metals [12], while the high price and possibility of producing secondary pollution are limited to application.

Biochar has an excellent adsorption performance because of its large specific surface area, loose and porous structure and rich functional groups [13,14]. Therefore, it is deemed as an emerging adsorbent in wastewater treatment, soil remediation, gas storage and separation [15,16]. Besides, it can also be devoted to manufacturing clean energy, partially replacing fossil fuels and plays a catalysts role to reduce greenhouse gas emissions [17]. Biomass feedstocks are mainly derived from agricultural waste and forest residue, wood chips, algae, sewage sludge, and animal manure [18,19]. The type of most widely used plant-based carbon feedstocks has received considerable attention by its properties. Notwithstanding accruing evidence supporting biochar is conducive to environmental remediation [20,21], little is known about how biochar theoretically achieve removal of Pb(II) from wastewater [22,23]. In this case, this was accredited that the involvement of surface functionalization technology can enhance the affinity to the target pollutants and then improve adsorption performance [24,25].

β-Cyclodextrin (β-CD), a harmless cyclic oligosaccharide macromolecule [26], is a particular framework with hydrophilic surface and hydrophobic inner cavity, making it to form complex compounds with organic pollutants and metal ions through host-guest complexation [27]. Most importantly, β-CD is constantly loaded on insoluble substances due to its external hydrophilic hydroxyl and acid-base stability. Hence, the cross-linked composite of β-CD has received extensive attention in the field of water pollution control [28]. For instance, composites using β-CD and chitosan crosslinked to glutaraldehyde and ethylenediamine tetraacetic acid dihydride achieved satisfactory results in experiments with simultaneous chelation of Pb^{2+} and acidic red dyes [29]. Chelates of β-CD crosslinked with rice husk-based biochar to form a network of materials with Pb^{2+} and bisphenol A or methylene blue have been reported to have significant adsorption effects [1–30]. Thus, the coupling of β-CD and biochar can simultaneously enhance the compatibility of cyclodextrin cavity guest to the functional groups and the hydrophilicity of composite. [31]. Whereas, few researches have been conducted on making use of environmental friendly glutaraldehyde as a crosslinker to graft β-CDs onto sycamore leaf-based biochar to remove Pb(II) from water. Therefore, the objectives of this study were to (1) synthesize the β-BC utilizing the chemical crosslinking of β-CD and sycamore leaf-based biochar, (2) analyze the properties of adsorbents using scanning electron microscopy (SEM), Brunauer–Emmett–Teller (BET) and Fourier-transform infrared spectroscopy (FTIR) as well as X-ray diffraction (XRD), (3) explore removal mechanism of Pb^{2+} adsorption onto adsorbents by means of the performance of using batch adsorption experiments in water. The results wish to provide more information for the evaluation of environmental behavior and toxicological effects of Pb^{2+} in aquatic environments.

2. Materials and methods

2.1. Materials and reagents

Chemical reagents including lead nitrate (≥99%), β-cyclodextrin (98%), glutaraldehyde (25% aqueous solution), and sodium hydroxide (granular, ≥96%) were obtained from Shanghai Hu Trial Chemical Co., (Shanghai, China). Sycamore leaves were gathered in Wuhan, Hubei province of China, which are washed with deionized water until the surface has no impurities, placed in an oven at 80°C to dry to invariable weight, ground into powder, then sealed in a dry environment. In order to prepare the Pb(II) stock solution, the appropriate amount of lead nitrate solids were weighed and dissolved in deionized water to obtain concentration of 50 mg L^{-1}.

2.2. Adsorbents

Anaerobic pyrolysis technology is used to produce sycamore leaf-based biochar. The pulverescent sample was constantly pyrolyzed at 500°C in a tube furnace for 120 min under N_2 environment at a heating rate of 10°C/min. Thus, the raw biochar was gained and named as BC. The β-CD functionalized BC was acquired using glutaraldehyde (25% solution) as a crosslinker, which is coupled with sycamore leaf-based biochar. 4 g β-CD and 4 mL glutaraldehyde were added to 200 mL of sodium hydroxide solution (7% w/v) and the solution was obtained after thorough churn. Moreover, 1.2 g of biochar was added to the solution, stirred and mixed at 200 rpm for 12 h and later filtrated to achieve solid–liquid separation. Subsequently, the separated solids were repeatedly washed with deionized water to neutrality, then dried in a vacuum oven at 80°C. Finally, the β-CD grafted biochar was synthesized and abbreviated as β-BC.

2.3. Characterization

Surface topography of samples was characterized by (SEM, FEI Corporation of the United States). The Brunauer–Emmett–Teller method (BET, Thermo Fisher Scientific, USA) was used to detect the pore size, pore volume and specific surface area of adsorbents, and the relevant nitrogen adsorption and desorption curve was achieved. Fourier-transform infrared spectroscopy (FTIR, Thermo Fisher Scientific, USA) measured the FTIR spectrum of adsorbents within the range of 4,000–400 cm^{-1}. The D8 Advance Eco X-ray diffractometer of BRUKER was used to analyze the crystalline structure before and after biochar modification. The Zeta potential analyzer (Malvern, UK) was used to determine the potential points of biochar at different pH values.

2.4. Batch adsorption experiments

A stock solution of Pb^{2+} with a concentration of 1 g/L was prepared by dissolving an appropriate amount of lead chloride in distilled water. Batch experiments were

conducted in 100 mL Erlenmeyer flasks containing 50 mL synthetic solution of Pb^{2+}. To study the kinetics adsorption of Pb^{2+} by sorbents, samples were collected at different time intervals (1 min, 5 min, 10 min, 15 min, 30 min, 45 min, 1 h, 1.5 h and 2 h). The isotherm adsorption experiment was performed in different Pb concentrations (50, 60, 70, 80, 90, and 100 mg L^{-1}) and sampling time (2 h) were applied. The investigated factors were solution pH (2–6), initial Pb^{2+} concentration (50–100 mg/L), β-BC dosage (0.01–0.06 g) and Cd^{2+} concentrations (50–100 mg/L). The pH of the aqueous medium was adjusted with NaOH (1 mol/L) or HCl (1 mol/L) solution.

Each experimental run was conducted in triplicate using agitation speed of 200 rpm at a room temperature of 25°C ± 1°C. After a certain time, the with-drawn samples were filtered using 0.45 μm aquatic polyethersulfone, and the filtrate was collected and stored in plastic bottles for further analysis. The residual Pb(II) in solutions was determined by flame atomic absorption spectrophotometer (Jena, Germany).

2.5. Analysis methods

The loading of Pb^{2+} adsorbed in aqueous could be calculated as adsorption capacity and removal percentage at time t by the following two formulas.

$$q_t = \frac{\left(C_0 - C_t\right)V}{m} \tag{1}$$

$$R\% = \frac{C_0 - C_t}{C_0} \times 100\% \tag{2}$$

where q_t (mg g^{-1}) is the adsorption capacity and R% is the removal percentage for pollutant, C_0 (mg L^{-1}) is the initial metal ion concentration in solution, C_t (mg L^{-1}) is the metal concentration at time t in min, V is the volume of adsorbate and m is the mass (g) of the adsorbent.

Calculate and process data using Microsoft Excel 2021 software, Graphical analysis using Origin 2019 software, SPSS 27.0 were used to perform a one-way ANOVA on the data, and $P < 0.05$ indicates a significant difference.

2.6. Models for kinetics

Kinetics data were prior fitted with the pseudo-first-order model (PFO) [32], the pseudo-second-order model (PSO) [33], and the Weber–Morris kinetic model [34], the relevant nonlinear equation are Eqs. (3) and (4) and the linear equation is Eq. (5) respectively:

$$q_t = q_e\left[1 - \exp\left(-k_1 t\right)\right] \tag{3}$$

$$q_t = \frac{q_e^2 k_2 t}{q_e k_2 t + 1} \tag{4}$$

$$q_t = k_{ip} t^{0.5} + C \tag{5}$$

where q_t is the equilibrium adsorption capacity (mg g^{-1}); k_1 is the rate constant of the pseudo-first-order kinetic model (min^{-1}); k_2 is the rate constant of the pseudo-second-order kinetic model (g mg^{-1} min^{-1}); K_{ip} is the diffusion rate constant within the particle (mg g^{-1} $min^{-1/2}$); t is the adsorption time (min).

2.7. Models for isotherm

The adsorption equilibrium data was processed in accordance with the well-known Langmuir model [35], Freundlich model [36] and Temkin model [37], where the mathematical nonlinear expressions is Eqs. (6)–(8), respectively:

$$q_e = \frac{q_m k_L C_e}{1 + k_L C_e} \tag{6}$$

$$q_e = k_F C_e^{1/n} \tag{7}$$

$$q_e = \frac{RT\ln\left(k_T C_e\right)}{b_T} \tag{8}$$

where q_m (mg g^{-1}) is the maximum adsorption capacity of the adsorbent, C_e (mg L^{-1}) is the target contaminant concentration in solution at equilibrium; k_L, k_F and k_T are the adsorption coefficients of Langmuir, Freundlich and Temkin models, respectively; $1/n$ is the intensity parameter for adsorbent. R (8.314 J/mol·K) is universal gas constant; T (298 K) is the absolute temperature; b_T is the Temkin constant associated with adsorption heat.

3. Results and discussion

3.1. Adsorbent of physico-chemical properties on surface

SEM images were viewed as a distinct method to observe the morphologies of BC and β-BC. Overarchingly, there was pervasively amorphous tissue, which were adhered to flaky crystals structures of BC and β-BC based on Fig. 1. Specifically, partial and ordered lamellar tissue were distinctly found on the wrinkled surface of BC (Fig. 1b), while via the combined treatment of NaOH penetration and β-cyclodextrin crosslinking, the surface of β-BC was mostly lumpy debris and attached a large number of fine solid particles (Fig. 1d). Owing to the surface of β-BC has concurrently exhibited irregular and small solid block structure, making the internal structure more diverse, which was supported that biochar is in favor of adsorption [38]. Compared with some similar adsorbents made of lignin, the surface morphology of β-BC has no obvious holes and cavity structures, which may be related to the pre-treatment method and temperature [12–14]. Therefore, the higher specific surface area of β-BC provided additional active sites to Pb^{2+}, resulting in pore-filling [39]. Table 1 clearly contrasted the specific surface area, total volume, microporous volume, and pore size of the two materials. Compared with BC, the slight decline appeared in S_{BET} and

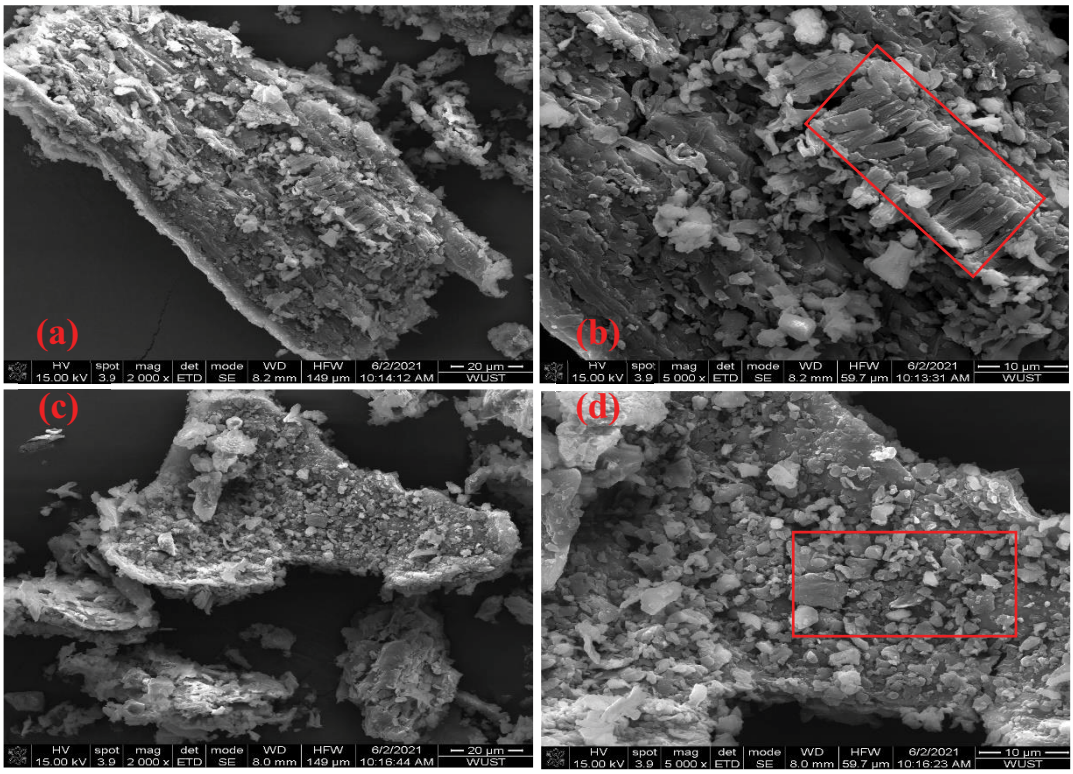

Fig. 1. SEM images of BC (a,b) and β-BC (c,d).

Table 1
Porous structure parameters of BC and β-BC

Samples	S_{BET} ($m^2\ g^{-1}$)	V_{tot} ($cm^3\ g^{-1}$)	V_{mic} ($cm^3\ g^{-1}$)	D_p (nm)
BC	4.69	0.0099	0.0004	8.48
β-BC	4.57	0.0062	0.0013	5.41

V_{tot}, (decreased by 0.12 $m^2\ g^{-1}$ and 0.0037 $cm^3\ g^{-1}$, respectively), D_p reduced from 8.48 to 5.41, whereas, V_{mic} increased by 3.25 times.

The N_2 adsorption/desorption isotherms and pore size distribution of BC and β-BC were exhibited in Figs. 2a–c. Judging by the nitrogen adsorption isotherms of IUPAC, BC was a type II isothermal curve with an H_3 hysteresis loop, which indicated that the pore structure was fairly irregular, and there may be a flat slit structure, cracks and wedge structures; while β-BC was III isothermal curve with an H_4 hysteresis loop, which was a multi-layer adsorption mesoporous material, most of which had slit holes with flake particle accumulation. Furthermore, within the scope of P/P_0 = 0–0.5, adsorption got ahead of desorption, but β-BC was an exception that could be attributed to the micropore-filling [40]. In addition, it was distinguished that materials desorption performance was superior regarding to the capacity of nitrogen adsorption/desorption, which was inferred that mesoporous or macroporous structure emerged in the range of P/P_0 = 0.5–1.0. Otherwise, the results shown in Fig. 2c also depicted the pore size distributions of BC and β-BC. The pore diameter of BC mainly focused on micropore range (4–27 nm), the pore size distribution of β-BC displayed increasing with diameter growth. Although, the specific surface area of the modified resembled the original, the adsorption capacity of β-BC could be expected to theoretically surpass that of BC. The probable explanation was the modification for β-BC with β-Cyclodextrin partly increased the amount of –OH and –COOH groups on surface, as well as host-guest interaction in cavity.

FTIR measurements were mainly observed to confirm the functional groups of four materials from 3,735 to 561 cm^{-1} as shown in Fig. 2d. The peak of about 3,425 cm^{-1} was stretching vibration represented the bonding water and nitrogen-hydrogen bonds, implied the presence of the $–NH_3$ and O–H groups in the whole materials [41]. Regarding BC, the characteristic peaks of about 1,729 cm^{-1} correspond to the telescopic vibration of C=O or C=C, where the peaks of about 1,600 and 1,463 cm^{-1} were crucial symbols of the aromatic hydrocarbon skeleton [41], and the peak of about 2,927 cm^{-1} ascertained the C–H bond in alkanes and aromatic hydrocarbons [42]. Relatively speaking, the spectrum of β-BC had a peak at 1,603 cm^{-1}, which became significantly flattened. It was distinguished that C–O or C–O–C telescopic vibration peak with a wavelength of 1,137–1,195 cm^{-1}, which was due to the dehydration reaction caused by –CHO and C–OH [43], indicating that β-cyclodextrin and BC were successfully crosslinked by glutaraldehyde. Furthermore, the curve after adsorption showed

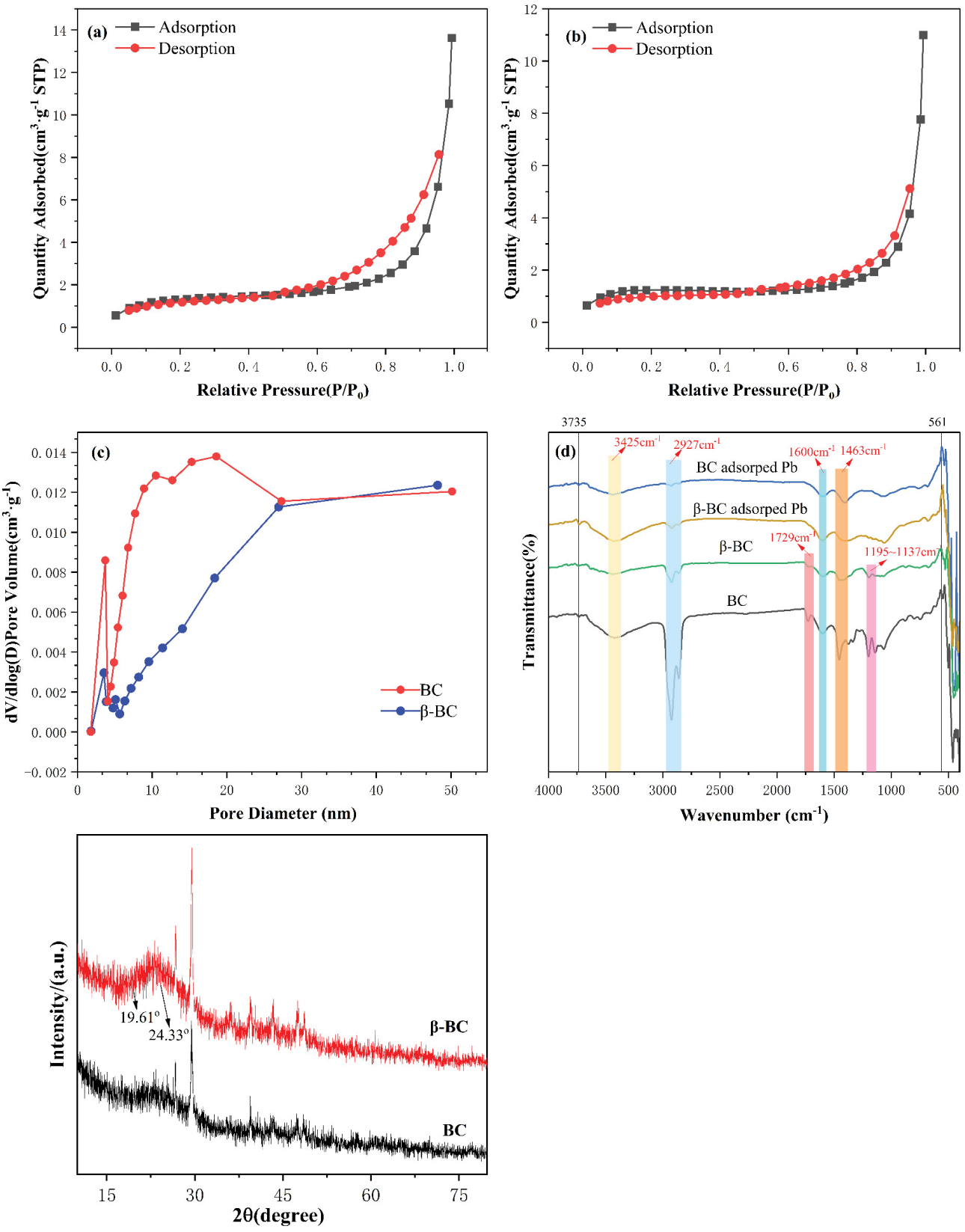

Fig. 2. The N_2 adsorption/desorption isotherms (a,b) and the pore-size distribution (c) of BC and β-BC; FTIR spectra of BC, and β-BC and adsorbed Pb(II), respectively; XRD patterns of BC and β-BC.

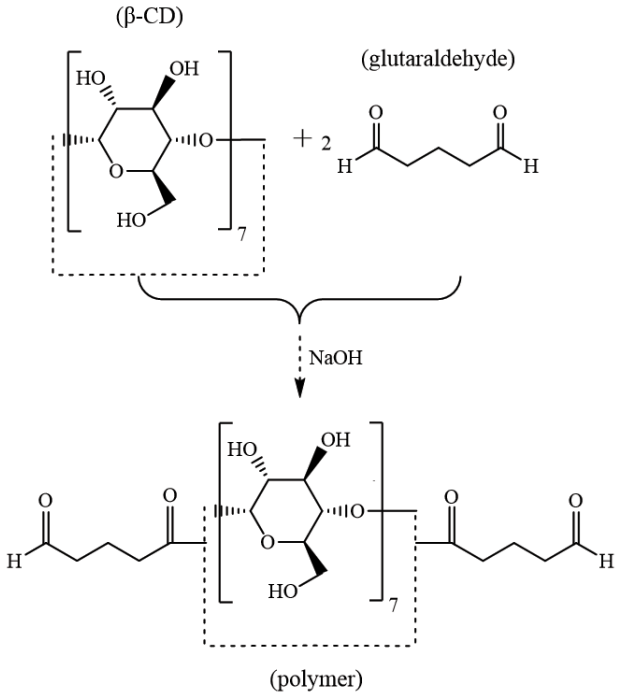

Fig. 3. Dehydration reaction of β-cyclodextrin with glutaraldehyde.

the peak intensity of O–H was slightly weaker than BC, the C–H peak of saturated alkanes moderated, proved that O–H and saturated alkanes form complexes with Pb^{2+} (Fig. 3). In addition, the right shift of C=O or C=C characteristic peak telescopic vibration of BC and β-BC at about 1,600 cm^{-1} after adsorption and the strong vibration of 561 cm^{-1} could determine the occurrence of halogen elements.

XRD was applied to analyze the crystal structure of BC and β-BC based on Fig. 2e. The characteristic peaks at 2θ = 12.43°, 14.71°, 15.30°, 17.06°, 19.61°, 21.12°, 22.64°, 24.33° and 27.12° were considered as β-CD [44]. The structure of β-BC surface was changed, and it was evident that the characteristic peaks at 26.72° and 29.46° converted to sharp and intense peaks. In addition, corresponding peaks of β-CD (2θ = 19.61° and 24.33°) could be found, indicating that β-CD was successfully loaded onto β-BC by glutaraldehyde crosslinking.

3.2. Adsorption properties of β-BC

3.2.1. Effect of β-BC initial pH values

As shown in Fig. 4a, the modified material of pH_{pzc} descended, pH_{pzc} = 2.82 of BC and pH_{pzc} = 2.14 of β-BC. The pH had a significant effect on the adsorption capacity of β-BC adsorption Pb^{2+} ($P < 0.05$). When the pH = 2, β-BC had almost no adsorption effect on Pb^{2+}; but when the pH rose to 3, the adsorption capacity had increased significantly to 47.61 mg g^{-1}, and then maintained a minor lessening with the augment of pH. When the solution pH was less than pH_{pzc} (2.14), the β-BC surface was positively charged because of protonation, which resulted chemical reactions in solution were mainly dominated by H^+ [45]. While pH was greater than pH_{pzc}, β-BC was negatively charged for deprotonation [19], and thereupon the surface produced a fierce electrostatic attraction on Pb^{2+} [46]. Meanwhile, the H^+ concentration in solution gradually declined, which was detrimental to electrostatic adsorption. In brief, the results proved β-BC had excellent Pb^{2+} removal ability, which potentially explained the following points: (1) the mechanism of adsorption by β-BC was electrostatic action under acidic conditions; (2) the presence of hydrogen bonds also warrant attention when Pb^{2+} was adsorbed; and (3) through intense host-guest interaction of β-BC. In summary, although the charged properties of β-BC surface changed with pH, the adsorption capacity of Pb^{2+} could remain stable within a specific pH range.

3.2.2. Effect of initial concentration of Pb^{2+}

For the initial concentration of the adsorbent, the adsorption of BC and β-BC on Pb^{2+} increased with significant effect ($P < 0.05$). With the initial Pb^{2+} concentration in constant 10 mg L^{-1} increments from 50 to 100 mg L^{-1}, the adsorption capacity of Pb^{2+} by BC and β-BC were increased stepwise, while the adsorption efficiency was gradually declined as can be seen from Fig. 4b. We further noted that when the initial preparation of Pb^{2+} was 50 mg L^{-1}, the adsorption performance was well-performing, where the adsorption capacity was close and the adsorption efficiency exceeded 90%, after that the difference was even more pronounced. When the Pb^{2+} concentration ascended to 100 mg L^{-1}, the adsorption capacity and efficiency of β-BC and BC reached 151.2 mg g^{-1}, 61.11%, and 120.22 mg g^{-1}, 25.45%, respectively. The consequences were restricted to the amount of adsorption sites and cavity structures and may also be due to physico-chemical property of adsorbents outer surface created complexes with Pb^{2+} [47]. However, β-BC had more mesoporous and active groups such as hydroxyl, carboxyl, alcohol group. [48], caused a major growth to remove Pb^{2+} under condition of identical adsorbent mass.

3.2.3. Effect of β-BC dosage

Fig. 4c presents the quantitative results of adsorption performance of different β-BC dosage for Pb^{2+} removal. The amount of adsorbent had a significant effect on the adsorption results of β-BC adsorption of Pb^{2+} ($P < 0.05$). When the amount of dosing increased from 0.01 to 0.06 g, the adsorption effect was remarkable, reflecting that the adsorption capacity decreased from 81.93 to 20.67 mg g^{-1}, and the removal efficiency increased from 66% to 99%. Moreover, the maximum removal efficiency had achieved when the dosage was 0.05 g. Concretely, after the amount of adsorbent was increased from 0.01 to 0.02 g, the adsorption capacity was reduced by 22.4 mg g^{-1}, whereas the removal efficiency increased by 29%, which was explained that increase in adsorbent dose not only enlarged the adsorption surface area, but also aggrandized the number of functional groups involved in adsorption. Therefore, the activated surface site of β-BC was in a low saturation state and a wealth of Pb^{2+} concentration, facilitating the adsorption on preliminary stage. Afterwards, with the increase of the dosage, the adsorption capacity decreased quantitatively, whereas the adsorption

efficiency remain basically unchanged. It was possibly owing to the exorbitant suspended adsorbent density, resulting in the adsorbent had stuck to each other and made the area in contact with the solution was reduced, thereby diminishing the proportion of the effective adsorption surface [49]. Until the amount of adsorbent was greater than a certain value, the surface adsorption capacity of β-BC was close to saturated, and finally inclined to be balanced.

3.3. Adsorption kinetics models

Fig. 4d and Table 2 shows the fitting results and related parameters of the PFO kinetics model and the PSO kinetics model simulation of BC and β-BC, respectively. The BC and β-BC adsorption to Pb^{2+} evidently reinforced followed adsorption time was prolongated, and finally levelling-off. BC and β-BC attained the adsorption equilibrium for about 30 min and 15 min, and the maximum adsorption amount was 48.44 and 52.4 mg g^{-1}, severally. For BC, the correlation coefficient of the PFO was greater than the PSO, and the fitting of the PFO calculated that the equilibrium adsorption amount of Pb^{2+} (q_e = 47.02 mg g^{-1}) was in proximity to the experimental data. This testified that the adsorption of BC to Pb^{2+} was more in line with the PFO kinetics model, indicating that BC was a single-molecule adsorption process dominated by physical adsorption. Conversely, the PSO kinetics correlation coefficient of β-BC was larger than the PFO, and it was speculated that β-BC adsorption to Pb^{2+} was more in accordance with the PSO kinetics model dominated by chemical multilayer adsorption.

To further comprehend BC and β-BC of adsorption rate on removal of Pb^{2+}, the Weber–Morris kinetic model was used to fit the experimental data, as can be seen from Fig. 4e. The fitting lines revealed a three-segment non-linear plot as well as the fitting coefficients of β-BC were more than 0.9, which indicated that the adsorption of Pb^{2+} by β-BC was a continuous segmented process. The linear adsorption in the first stage was prone to surface diffusion, the second stage was the intragranular diffusion process, and the third stage was the equilibrium dynamic process of adsorption and desorption [50]. With the help of these observations, material transfer and physico-chemical reactions during

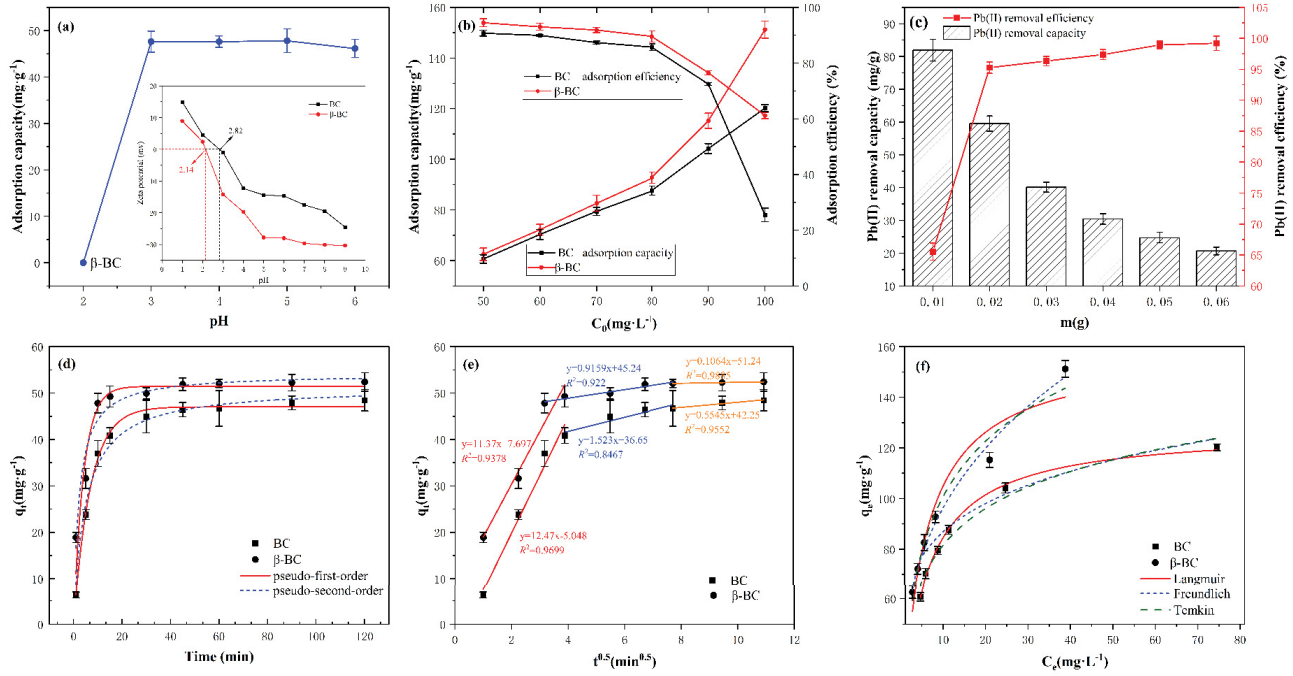

Fig. 4. Effects of pH by β-BC (a), effects of initial concentration of Pb^{2+} (b), effects of dosage for β-BC (c), adsorption kinetics fitting curves for BC and β-BC (d), fitting curves of Weber–Morris model (e), and fitting curves of isothermal models for BC and β-BC (f) (T = 25°C; pH = 6).

Table 2
Parameters of adsorption kinetics

	Pseudo-first-order equation			Pseudo-second-order equation		
	q_e (mg g^{-1})	k_1 (min^{-1})	R_1^2	q_e (mg g^{-1})	k_2 (g mg^{-1} min^{-1})	R_2^2
BC	47.02 (±0.4586)	0.1437 (±0.0064)	0.9949	51.36 (±1.173)	0.0040 (±0.0006)	0.9828
β-BC	51.44 (±1.477)	0.2416 (±0.0398)	0.9101	54.17 (±1.457)	0.0082 (±0.0017)	0.9417

adsorption that can be applied to interpret the adsorption of Pb^{2+} was identified.

3.4. Adsorption isotherm models

Fig. 4f and Table 3 shows the fitting results and related parameters of the BC and β-BC adsorption to Pb^{2+} isothermal models, respectively. Evidently, the rise of equilibrium concentration was rewarding to the adsorptive capacity. Under the action of the driving force generated by the concentration gradient, the absorption of Pb(II) increases with the increase of concentration [3–19]. Besides, the affinity of β-BC for Pb(II) was higher than BC, indicating that β-BC was the core component responsible for capturing Pb(II) [2]. The correlation coefficient of the Langmuir model (R^2 = 0.9967) fitted to BC was superior to the Freundlich model (R^2 = 0.9282) and the Temkin model (R^2 = 0.9697). The fitted q_m = 151.2 mg g^{-1} was in close proximity to the q_{max} = 158.9 mg g^{-1} measured in practice, it higher than 120.22 mg g^{-1} of BC. Table 4 listed the comparison of the adsorption capacity of β-CD modified various adsorbents to Pb^{2+}. This indicated that β-BC was an excellent adsorbent for purification of Pb(II) in wastewater. The Langmuir model was more appropriate for delineating the relationship between adsorption and concentration for Pb^{2+}. Consequently, it was also declared that the adsorption was ascribed to the single-layer surface adsorption process. Additionally, the correlation coefficient fitted by the Freundlich model (R^2 = 0.9847) for adsorption of β-BC preceded the Langmuir model (R^2 = 0.916) and the Temkin model (R^2 = 0.9644), which demonstrated that the adsorption process accorded with the monolayer chemical adsorption process. The adsorption of BC and β-BC on Pb^{2+} were fitted with the Temkin model, manifesting that the adsorption activation energy had changed, thereby proving the involvement of chemisorption throughout the process. 1/n was less than 1, indicating a strong monolayer adsorption in existence in the process onto materials.

3.5. Competitive adsorption of Cd(II)-Pb binary system

This experiment investigated that when the initial pH was about 6, the high-performance β-BC was adsorbed to diverse Pb^{2+} concentrations in the Cd^{2+} interference from 50 to 100 mg L^{-1} (concentration gradient of 10 mg L^{-1}), whereupon its synchronous adsorption effectiveness was calculated in Cd(II)-Pb binary system and was calculated as:

$$R_{q,i} = \frac{q_{b,i}}{q_{u,i}} \tag{9}$$

where $q_{b,i}$ (mg g^{-1}) and $q_{u,i}$ (mg g^{-1}) are corresponding to adsorption capacities of binary and unitary systems, respectively, based on same Pb^{2+} original concentration.

As shown in Fig. 5a and b, the adsorption capacity of Pb^{2+} enhanced with lead or cadmium in monolithic and binary solution systems. However, the adsorption capacity

Table 3
Fitting parameters of isothermal adsorption models

	Langmuir			Freundlich			Temkin		
	q_m (mg g^{-1})	k_L (L mg^{-1})	R^2	k_F ($mg^{1-1/n}$ g^{-1} $L^{1/n}$)	1/n	R^2	k_T (L g^{-1})	b_T	R^2
BC	127.4 (±1.374)	0.1944 (±0.0073)	0.9967	57.58 (±0.3576)	0.1772 (±0.0541)	0.9282	4.608 (±1.534)	116.8 (±9.259)	0.9697
β-BC	158.9 (±11.81)	0.1915 (±0.0427)	0.916	45.85 (±2.37)	0.3201 (±0.1764)	0.9847	2.319 (±0.6266)	77.67 (±6.682)	0.9644

Table 4
Comparison of heavy metal adsorption capacities by β-CD modified various adsorbents

Adsorbent	Pollutant	$q_{e,max}$ (mg g^{-1})	Removal mechanism	References
β-cyclodextrin pyrolysis product	Cd(II)	1,237.42	Complexation	[20]
β-CD/PLGA hybrid modified biochar	Cr(VI)	197.21	Electrostatic interaction	[21]
β-CD modified rice husk biochar	Pb(II)	240.13	Complexation, electrostatic interactions	[1]
β-CD functionalized rice straw biochar	Pb(II)	131.24	Physical diffusion, exchange of ionizable protons/cations, and complexation	[23]
β-CD functionalized palm biochar	Pb(II)	118.08	Ion exchange, chemical bonding	
β-CD-loaded zeolite	Pb(II)	175.25	Diffusional movement, chemical exchange of ionizable protons or cations, and chemical bonding	[31]
	Cd(II)	93.06		
β-CD-loaded vermiculite	Pb(II)	126.35		
	Cd(II)	68.65		
β-CD functionlized sycamore leaf-based biochar	Pb(II)	151.2	Electrostatic action, complexation, hydrogen bonding of a wealth of oxygenated groups, and host-object interaction	This work

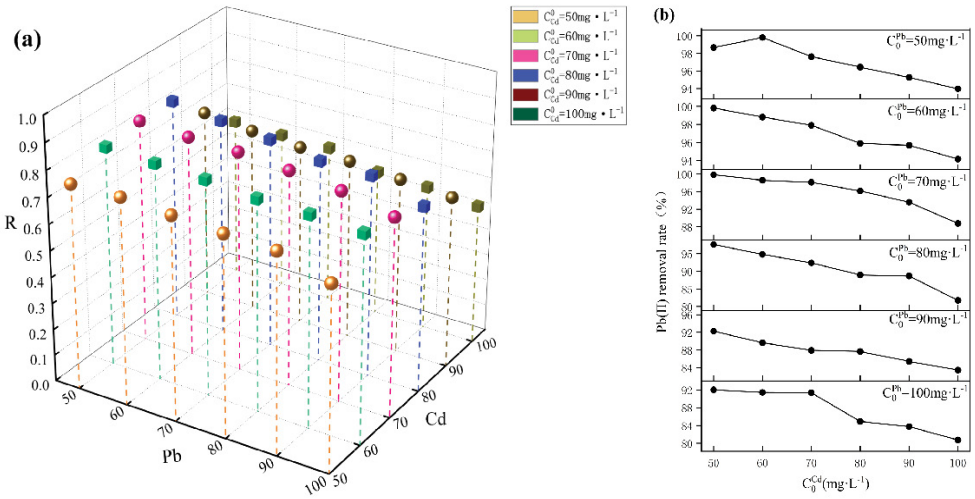

Fig. 5. Bivariate adsorption of β-BC to Pb(II) (a) and the removal rate of Pb(II) in binary systems (b) (C_0^{Pb} and C_0^{Cd} = 50~100 mg/L; T = 25°C; pH = 6; m = 0.05).

of Pb^{2+} in a single system excelled in a binary system. Careful observation showed that $0 < R < 1$, indicating that Cd^{2+} had exerted an inhibition influence on Pb^{2+} in the binary system solution. When the concentration of Cd(II) gradually increased, the R value decreased, particularly ΔR was the largest when Pb^{2+} initial concentration was 80 mg L^{-1}, and R_{max} = 0.85 was evaluated under C_0^{Pb} was 70 mg L^{-1} and C_0^{Cd} [TS 3] was 50 mg L^{-1} conditions.

The above results demonstrated that the co-existence of two metal ions was capable to stimulate competition for active adsorption sites on the surface of β-BC. Moreover, the corresponding Cd^{2+} concentration of R_{max} had an expressly intense inhibiting effect on Pb^{2+}, which may be that Cd^{2+} and Pb^{2+} were affected by other factors except the competitive adsorption site. Whether it was a mono- or multi-ingredient system, the increase in Pb^{2+} concentration allows β-CD to be encapsulated into the cavity by host-guest complexation and can provide potential π–π stacking interaction with Pb^{2+} or Cd^{2+} to progress adsorption performance in the presence of supramolecular interactions and aromatic backbones. Another explanation was that Pb^{2+} and Cd^{2+} are associated with ionic radius (r_{ion}), factually, r_{ion} (Pb) and r_{ion} (Cd) are 1.20 and 0.97 Å, respectively [51]. This was acceptable to Cd^{2+} and is prone to bind to the active site, resulted in the adsorption of Pb^{2+} was restricted by the spatial thrombotic hindrance, which reflected the antagonism/inhibition of the two metal ions at the same active receptor site. There are other influencing factors that are beneficial to competitive adsorption capacity for Pb. It was estimated that Pb had a maximum atomic weight (207.2), strong electronegativity (Pb^{2+} (2.33) > Cd^{2+} (1.69)) [52], which made it possible for Pb^{2+} to be bound by carboxyl, aldehyde, or ether groups β-BC. Apart from that, Saha et al. [53] believed that the negative logarithm of the first-order hydrolysis constant of Pb (7.8) was less than Cd (10.1), so the adsorption affinity of Pb was stronger. Heavy metal ions entering the β-BC pores need to dislodge the water film to undergo complexation, while the heat of hydration (1,500 kJ mol^{-1}) of Pb under Cd (1,826.7 kJ mol^{-1}) [54]. Hence, Pb^{2+} was more likely to dehydrate with β-BC chemical groups and be fixed. Lin et al. [55] believed that Pb forms intra-loop compounds through intra-cavity complexation, and the covalent bonds formed are more stable.

3.6. Removal mechanism

By the analysis of adsorption kinetics and isothermal models, the adsorption of Pb^{2+} in water by BC and β-BC is multifarious types of adsorption mechanisms that contain physical and chemical effects. The PSO kinetics model and the Freundlich isothermal model are more consistent with the changes in the adsorption rate and adsorption concentration of Pb^{2+} on the surface of β-BC. The explanation is that the adsorption surface of β-BC is not uniform in energy, which may be related to the addition of functional groups, including hydroxyl and amino groups, coated on the surface after biochar modification [20]. The large value of $1/n$ indicates the stronger the interaction between the adsorbent and the Pb^{2+}, mainly limited by the diffusion rate within the particles, indicated that polar functional groups may have chemical effects on β-BC and Pb^{2+}, including ion exchange and chelation reactions [23]. The experimental results of influencing factors emerged that the pH of the solution, the concentration of pollutants, the amount of β-BC and the competitive adsorption of Cd^{2+} to Pb^{2+}, certified that the adsorption of Pb^{2+} was affected in different aspects. The pH values could change the surface charge of adsorbents, and the high concentration of Cd^{2+} inhibited the adsorption of Pb. The mechanism may be that the hydroxyl group of β-CD enhanced the adsorption of heavy metal ions by interacting with metal ions, and when β-CD polymer was used as an absorbent, the metal with higher affinity had the ability to replace the less affinity metal, which lead to a decrease in metal removal efficiency [22]. With the increase of Cd^{2+} concentration in binary system, the migration rate of Pb^{2+} on the surface of biochar was observed to slow down, the finite adsorption site was occupied. These

trends are attributed to the different physico-chemical properties of the heavy metals lead and cadmium, which is consistent with previous studies [1–31].

Surface functional groups mainly control the adsorption of heavy metal ions on biochar. The cleavage products of β-CD at 500°C have a high adsorption capacity for Pb^{2+} [20]. This may be due to its rich oxygen-containing functional group, which can be complexed with Pb^{2+} to achieve the effect of adsorbing heavy metals. FTIR was used to further explore the interaction between biochar and heavy metals. The characteristic peak strength of hydroxyl (–OH) located around 3,425 cm^{-1} weakened, which implied that the –OH in BC and β-BC can be precipitated with Pb^{2+} to form $Pb_2(OH_3)Cl$ or $Pb(OH)_2$. Especially, the β-BC adsorbed Pb^{2+}, the characteristic peak strength of –OH was enhanced, which may be due to the hydrogen bond and Pb^{2+} involved in electron transfer to generat $Pb(OH)_2$ or $HPbO^{2-}$.The high O content of the functional group makes the β-BC have a higher CEC, especially carboxylic acid, which provided the cation exchange capacity of the material through ionizable proton/cation exchange [31]. BC at 2,927 cm^{-1} represented a strong peak of phenolic hydroxyl groups greatly weakened, which may have occurred ion exchange to form $(C_6H_6O)_2Pb$. After the adsorption of Pb^{2+} by β-BC, the C=O intensity increased, which may predicate that the carboxylic acid group was also involved in electrostatic adsorption, forming $(–COO)_2Pb$ and $(–COO)Pb^+$. The aromatic structure of C=C or –CH in biochar can be coordinated with cations by π bonds. After the adsorption of BC and β-BC, there was still a C=C group peak at 1,600 cm^{-1}, indicating that the π bond interacts with the cation, formed $C\pi\text{-}Pb^{2+}$ [56].

In addition to the above analyses, there are evidence that have been emphasized that the adsorption of heavy metals by β-BC may also include complexation and electrostatic adsorption. This was assigned to the presence of hydroxyl and carboxyl groups that could offer active sites to form more metal complexes. Furthermore, the essence of ion exchange was imputed the electrostatic action of negatively charged groups and positively charged heavy metal ions on the surface of biochar, which may be one of the most important mechanisms for biochar to adsorb heavy metals.

4. Conclusion

In this study, SEM and BET analysis showed that the modified biochar surface was significantly rough, with a slight decrease in specific surface area, total pore volume and average pore size, but the microporous area and micropore volume were 3.25 times that of BC. Further, FTIR analysis confirmed that the spectrum had a telescopic vibration peak at C–O or C–O–C at 1,137–1,195 cm^{-1} and occurred the dehydration reaction. It would be affirmed that β-cyclodextrin was successfully grafted onto sycamore leaf-based biochar (β-BC). Combined with the analysis of mathematical models, the adsorption of BC to Pb^{2+} was mostly physical adsorption, and the adsorption rate of pollutants was mainly affected by the diffusion within the particles. The adsorption of β-BC to Pb^{2+} was mostly motivated by chemical adsorption, and the adsorption mechanism of β-BC was more complex. In addition, BC and β-BC can also interact with cations through π bonds. Univariate adsorption experiments showed that the modified biochar had better adsorption efficiency. The amount of biochar, the initial pH, the initial concentration, and the contact time all had a significant impact on the removal effect of heavy metals. Binary adsorption experiments indicated that the concentration of heavy metal Cd^{2+} inhibited the adsorption of Pb^{2+} on biochar, which is related to the factors such as ion radius and electronegativity. Combined with characterization, functional groups such as hydroxyl (–OH) and carboxyl group (–COOH) in biochar played a dominant role in the adsorption. The adsorption of heavy metals by β-BC mainly includes electrostatic effect, cationic-π bond hybridization, coprecipitation and ion exchange.

Disclosure statement

No potential conflict of interest was reported by the author(s).

Acknowledgments

This research was financially supported by the open research program of Hubei Key Laboratory for Efficient utilization and agglomeration of metallurgic mineral resources, Wuhan University of Science and Technology (Grant No. 2020zy003) and Wuhan Science and Technology Planning Project (Grant No. 2020020601012274).

References

[1] J. Qu, M. Dong, S. Wei, Q. Meng, L. Hu, Q. Hu, Y. Zhang, Microwave-assisted one pot synthesis of β-cyclodextrin modified biochar for concurrent removal of Pb(II) and bisphenol A in water, Carbohydr. Polym., 250 (2020) 117003, doi: 10.1016/j.carbpol.2020.117003.

[2] L. Tian, K.B. Fu, S. Chen, J. Yao, L. Bian, Comparison of microscopic adsorption characteristics of Zn(II), Pb(II), and Cu(II) on kaolinite, Sci. Rep., 12 (2022) 1–13.

[3] J. He, Y. Li, C. Wang, K. Zhang, D. Lin, L. Kong, J. Liu, Rapid adsorption of Pb, Cu and Cd from aqueous solutions by β-cyclodextrin polymers, Appl. Surf. Sci., 426 (2017) 29–39.

[4] D. Georgouvelas, H.N. Abdelhamid, J. Li, U. Edlund, A.P. Mathew, All-cellulose functional membranes for water treatment: adsorption of metal ions and catalytic decolorization of dyes, Carbohydr. Polym., 264 (2021) 118044, doi: 10.1016/j.carbpol.2021.118044.

[5] A.R. Khan, F.U. Hajira Tahir, U. Hameed, Adsorption of methylene blue from aqueous solution on the surface of wool fiber and cotton fiber, J. Environ. Manage., 9 (2005) 29–35.

[6] M. Imamoglu, H. Şahin, Ş. Aydın, F. Tosunoğlu, H. Yılmaz, S.Z. Yıldız, Investigation of Pb(II) adsorption on a novel activated carbon prepared from hazelnut husk by K_2CO_3 activation, Desal. Water Treat., 57 (2016) 4587–4596.

[7] T. Rasheed, F. Kausar, K. Rizwan, M. Adeel, F. Sher, N. Alwadai, F.H. Alshammari, Two dimensional MXenes as emerging paradigm for adsorptive removal of toxic metallic pollutants from wastewater, Chemosphere, 287 (2022) 132319, doi: 10.1016/j.chemosphere.2021.132319.

[8] A. Jamshaid, A. Hamid, N. Muhammad, A. Naseer, M. Ghauri, J. Iqbal, N.S. Shah, Cellulose-based materials for the removal of heavy metals from wastewater–an overview, Chem. Bioeng Rev., 4 (2017) 240–256.

[9] S. Muthusaravanan, N. Sivarajasekar, J.S. Vivek, T. Paramasivan, M. Naushad, J. Prakashmaran, O.K. Al-Duaij, Phytoremediation of heavy metals: mechanisms, methods and enhancements, Environ. Chem. Lett., 16 (2018) 1339–1359.

[10] M. Imamoglu, A. Vural, H. Altundag, Evaluation of adsorptive performance of dehydrated hazelnut husks carbon for Pb(II) and Mn(II) ions, Desal. Water Treat., 52 (2014) 7241–7247.
[11] Ç. Özer, M. İmamoğlu, Isolation of nickel(II) and lead(II) from aqueous solution by sulfuric acid prepared pumpkin peel biochar, Anal. Lett., (2022) 1–13, doi: 10.1080/00032719.2022.2078981.
[12] M. Fawzy, M. Nasr, H. Nagy, S. Helmi, Artificial intelligence and regression analysis for Cd(II) ion biosorption from aqueous solution by *Gossypium barbadense* waste, Environ. Sci. Pollut. Res., 25 (2018) 5875–5888.
[13] M. Fawzy, M. Nasr, S. Helmi, H. Nagy, Experimental and theoretical approaches for Cd(II) biosorption from aqueous solution using *Oryza sativa* biomass, Int. J. Phytorem., 18 (2016) 1096–1103.
[14] M. Fawzy, M. Nasr, S. Adel, S. Helmi, Regression model, artificial neural network, and cost estimation for biosorption of Ni(II)-ions from aqueous solutions by *Potamogeton pectinatus*, Int. J. Phytorem., 20 (2018) 321–329.
[15] A.E. Creamer, B. Gao, Carbon-based adsorbents for post-combustion CO_2 capture: a critical review, Environ. Sci. Technol., 50 (2016) 7276–7289.
[16] F. Yang, Z. Xu, L. Yu, B. Gao, X. Xu, L. Zhao, X. Cao, Kaolinite enhances the stability of the dissolvable and undissolvable fractions of biochar via different mechanisms, Environ. Sci. Technol., 52 (2018) 8321–8329.
[17] J. Fang, L. Zhan, Y.S. Ok, B. Gao, Minireview of potential applications of hydrochar derived from hydrothermal carbonization of biomass, J. Ind. Eng. Chem., 57 (2018) 15–21.
[18] A. Colantoni, N. Evic, R. Lord, S. Retschitzegger, A.R. Proto, F. Gallucci, D. Monarca, Characterization of biochars produced from pyrolysis of pelletized agricultural residues, Renewable Sustainable Energy Rev., 64 (2016) 187–194.
[19] B. Chen, S. Chen, H. Zhao, Y. Liu, F. Long, X. Pan, A versatile β-cyclodextrin and polyethyleneimine bi-functionalized magnetic nano-adsorbent for simultaneous capture of methyl orange and Pb(II) from complex wastewater, Chemosphere, 216 (2019) 605–616.
[20] L. Ying, J. Liu, J. Li, J. Guo, Adsorption properties of β-cyclodextrin cracking products for Cd^{2+}, IOP Conf. Ser.: Earth Environ. Sci., 508 (2020) 012148, doi: 10.1088/1755-1315/508/1/012148.
[21] L. Jiang, S. Liu, Y. Liu, G. Zeng, Y. Guo, Y. Yin, X. Huang, Enhanced adsorption of hexavalent chromium by a biochar derived from ramie biomass (*Boehmeria nivea* (L.) Gaud) modified with β-cyclodextrin/poly(L-glutamic acid), Environ. Sci. Pollut. Res., 24 (2017) 23528–23537.
[22] H. Lyu, B. Gao, F. He, A.R. Zimmerman, C. Ding, J. Tang, J.C. Crittenden, Experimental and modelling investigations of ball-milled biochar for the removal of aqueous methylene blue, Chem. Eng. J., 335 (2018) 110–119.
[23] H.T. Zhao, S. Ma, S.Y. Zheng, S.W. Han, F.X. Yao, X.Z. Wang, K. Feng, β–cyclodextrin functionalized biochars as novel sorbents for high-performance of Pb^{2+} removal, J. Hazard. Mater., 362 (2019) 206–213.
[24] H. Ali, Biodegradation of synthetic dyes-a review, Water Air Soil Pollut., 213 (2010) 251–273.
[25] Y. Yang, L. Zeng, Z. Lin, H. Jiang, A. Zhang, Adsorption of Pb^{2+}, Cu^{2+} and Cd^{2+} by sulfhydryl modified chitosan beads, Carbohydr. Polym., 274 (2021) 118622, doi: 10.1016/j.carbpol.2021.118622.
[26] S. Kawano, T. Kida, K. Miyawaki, Y. Noguchi, E. Kato, T. Nakano, M. Akashi, Cyclodextrin polymers as highly effective adsorbents for removal and recovery of polychlorobiphenyl (PCB) contaminants in insulating oil, Environ. Sci. Technol., 48 (2014) 8094–8100.
[27] A. Alsbaiee, B.J. Smith, L. Xiao, Y. Ling, D.E. Helbling, W.R. Dichtel, Rapid removal of organic micropollutants from water by a porous β-cyclodextrin polymer, Nature, 529 (2016) 190–194.
[28] H. Liu, X. Cai, Y. Wang, J. Chen, Adsorption mechanism-based screening of cyclodextrin polymers for adsorption and separation of pesticides from water, Water Res., 45 (2011) 3499–3511.
[29] D. Wu, L. Hu, Y. Wang, Q. Wei, L. Yan, T. Yan, B. Du, EDTA modified β-cyclodextrin/chitosan for rapid removal of Pb(II) and acid red from aqueous solution, J. Colloid Interface Sci., 523 (2018) 56–64.
[30] Y. Liu, M. Liu, J. Jia, D. Wu, T. Gao, X. Wang, F. Li, β-Cyclodextrin-based hollow nanoparticles with excellent adsorption performance towards organic and inorganic pollutants, Nanoscale, 11 (2019) 18653–18661.
[31] S. Zheng, S. Xia, S. Han, F. Yao, H. Zhao, M. Huang, β-Cyclodextrin-loaded minerals as novel sorbents for enhanced adsorption of Cd^{2+} and Pb^{2+} from aqueous solutions, Sci. Total Environ., 693 (2019) 133676, doi: 10.1016/j.scitotenv.2019.133676.
[32] Y.S. Ho, G. McKay, Pseudo-second-order model for sorption processes, Process Biochem., 34 (1999) 451–465.
[33] Y.S. Ho, Review of second-order models for adsorption systems, J. Hazard. Mater., 136 (2006) 681–689.
[34] M. Alkan, Ö. Demirbaş, M. Doğan, Adsorption kinetics and thermodynamics of an anionic dye onto sepiolite, Microporous Mesoporous Mater., 101 (2007) 388–396.
[35] K.R. Hall, L.C. Eagleton, A. Acrivos, T. Vermeulen, Pore-and solid-diffusion kinetics in fixed-bed adsorption under constant-pattern conditions, Ind. Eng. Chem. Res., 5 (1966) 212–223.
[36] R.T. Yang, Adsorbents: Fundamentals and Applications, John Wiley & Sons, 2003.
[37] A. Ozaki, H.S. Taylor, M. Boudart, Kinetics and mechanism of the ammonia synthesis, Proc. Math. Phys. Eng. Sci., 258 (1292) (1960) 47–62.
[38] I. Saha, A. Ghosh, D. Nandi, K. Gupta, D. Chatterjee, U.C. Ghosh, β-Cyclodextrin modified hydrous zirconium oxide: synthesis, characterization and defluoridation performance from aqueous solution, Chem. Eng. J., 263 (2015) 220–230.
[39] Z. Luo, H. Chen, S. Wu, C. Yang, J. Cheng, Enhanced removal of bisphenol A from aqueous solution by aluminum-based MOF/sodium alginate-chitosan composite beads, Chemosphere, 237 (2019) 124493, doi: 10.1016/j.chemosphere.2019.124493.
[40] A.A. Faisal, S.F. Al-Wakel, H.A. Assi, L.A. Naji, M. Naushad, Waterworks sludge-filter sand permeable reactive barrier for removal of toxic lead ions from contaminated groundwater, J. Water Process. Eng., 33 (2020) 101112, doi: 10.1016/j.jwpe.2019.101112.
[41] H. Ge, J. Du, Selective adsorption of Pb(II) and Hg(II) on melamine-grafted chitosan, Int. J. Biol. Macromol., 162 (2020) 1880–1887.
[42] J. Li, G. Yu, L. Pan, C. Li, F. You, S. Xie, X. Shang, Study of ciprofloxacin removal by biochar obtained from used tea leaves, J. Environ. Sci. (China), 73 (2018) 20–30.
[43] Y. Sun, H. Li, G. Li, B. Gao, Q. Yue, X. Li, Characterization and ciprofloxacin adsorption properties of activated carbons prepared from biomass wastes by H_3PO_4 activation, Bioresour. Technol., 217 (2016) 239–244.
[44] M. Kundu, S. Saha, M.N. Roy, Evidences for complexations of β-cyclodextrin with some amino acids by ^{1}H NMR, surface tension, volumetric investigations and XRD, J. Mol. Liq., 240 (2017) 570–577.
[45] S. Iftekhar, V. Srivastava, M. Sillanpää, Enrichment of lanthanides in aqueous system by cellulose-based silica nanocomposite, Chem. Eng. J., 320 (2017) 151–159.
[46] S. Zhuang, Y. Liu, J. Wang, Covalent organic frameworks as efficient adsorbent for sulfamerazine removal from aqueous solution, J. Hazard. Mater., 383 (2020) 121126, doi: 10.1016/j.jhazmat.2019.121126.
[47] F.M. Mpatani, A.A. Aryee, A.N. Kani, Q. Guo, E. Dovi, L. Qu, R. Han, Uptake of micropollutant-bisphenol A, methylene blue and neutral red onto a novel bagasse-β-cyclodextrin polymer by adsorption process, Chemosphere, 259 (2020) 127439, doi: 10.1016/j.chemosphere.2020.127439.
[48] R. Zhao, Y. Wang, X. Li, B. Sun, C. Wang, Synthesis of β-cyclodextrin-based electrospun nanofiber membranes for highly efficient adsorption and separation of methylene blue, ACS Appl. Mater. Interfaces, 7 (2015) 26649–26657.
[49] N.C. Feng, X.Y. Guo, Characterization of adsorptive capacity and mechanisms on adsorption of copper, lead and zinc by

modified orange peel, Trans. Nonferrous Met. Soc. China, 22 (2012) 1224–1231.
[50] N. Kannan M.M. Sundaram, Kinetics and mechanism of removal of methylene blue by adsorption on various carbons-a comparative study, Dyes Pigm., 51 (2001) 25–40.
[51] L. Sellaoui, F.E. Soetaredjo, S. Ismadji, A. Bonilla-Petriciolet, C. Belver, J. Bedia, A. Erto, Insights on the statistical physics modeling of the adsorption of Cd^{2+} and Pb^{2+} ions on bentonite-chitosan composite in single and binary systems, Chem. Eng. J., 354 (2018) 569–576.
[52] J.X. Yu, L.Y. Wang, R.A. Chi, Y.F. Zhang, Z.G. Xu, J. Guo, Competitive adsorption of Pb^{2+} and Cd^{2+} on magnetic modified sugarcane bagasse prepared by two simple steps, Appl. Surf. Sci., 268 (2013) 163–170.
[53] U.K. Saha, S. Taniguchi, K. Sakurai, Simultaneous adsorption of cadmium, zinc, and lead on hydroxyaluminum-and hydroxyaluminosilicate-montmorillonite complexes, Soil Sci. Soc. Am. J., 66 (2002) 117–128.
[54] Y. Chen, H. Peng, R. Hou, S. Sun, F. Wang, Single and competitive adsorption of Pb(II) and Cd(II) onto modified peat, Appl. Chem. Ind., 2 (2019) 243–247.
[55] Q. Lin, S. Xu, A review on competitive adsorption of heavy metals in soils, Soils, 40 (2008) 706–711.
[56] N.F.A. Dsugi, A.A. Elbashir, Supramolecular interaction of moxifloxacin and β-cyclodextrin spectroscopic characterization and analytical application, Spectrochim. Acta, Part A, 137 (2015) 804–809.